Journal of Alloys and Compounds 515 (2012) 63–67

Contents lists available at SciVerse ScienceDirect

Journal of Alloys and Compounds

journal homepage: www.elsevier.com/locate/jallcom

Electrical properties of the arc-melted, layered-perovskite system $Nd_nTi_nO_{3n+2}$ with $n = 4.5–6.5$

E.J. Connolly[a,*], R.J.D. Tilley[b]

[a] Electronic Instrumentation Laboratory, Mekelweg 4, 2628 CD Delft, TU Delft, Netherlands
[b] School of Engineering, Cardiff University, P.O. Box 917, Cardiff CF2 1XH, UK

ARTICLE INFO

Article history:
Received 29 July 2011
Received in revised form 8 November 2011
Accepted 9 November 2011
Available online 18 November 2011

Keywords:
Rare earth alloys and compounds
Chemical synthesis
Electrical transport
X-ray diffraction

ABSTRACT

$Nd_nTi_nO_{3n+2}$, phases with n nominally 4.5, 5, 5.5, 6 and 6.5 have been prepared by the technique of arc-melting. As n is increased, (or, as oxygen is removed from $Nd_4Ti_4O_7$), there is a large decrease in the measured resistances, although the materials remained semiconducting/insulating. Values of activation energies E_a ranging from ~0.086 to 140 meV are observed and are similar to those observed for other isostructural layered systems. Although lattice parameters could not be extracted due to the multiphase nature of our samples, the results overall correlate with electron microscopy studies and with studies on isostructural materials. It is suggested that these materials may be useful in studying the electrical properties of 1-dimensional materials, as sensors, or possibly materials/systems with electric-field controlled charge carrier density.

1. Introduction

Perovskite oxide materials (ABO_3) are fascinating due to the range of properties they possess. Moreover, many closely related phases exist in which thin slabs of the "three dimensional" perovskite structure are joined by planes which, in effect, alter the stoichiometry of the material. When the slab interface is fixed and the slab thickness varies a homologous series of phases result. In these "two dimensional" phases the variation in properties becomes even more pronounced, ranging from ferroelectric insulators to high-T_c superconductors, including giant-magnetoresistive materials and one and two-dimensional metals [1–5].

The compounds $Nd_nTi_nO_{3n+2}$ form such a homologous series. Electron microscopy has shown that well-ordered $Nd_nTi_nO_{3n+2}$ phases with $n = 4$, 5, 6 can be prepared by the technique of arc-melting [6–9] as well as materials composed of ordered and disordered intergrowths with varying slab thickness. When the nominal value of the composition is greater than $Nd_6Ti_6O_{20}$, this latter structure coexisted with a non-stoichiometric perovskite phase with approximate composition $NdTiO_{3.15}$.

The $Nd_nTi_nO_{3n+2}$ phases have a crystal structure composed of n-octahedra-thick {1 1 0} slabs of perovskite-like material, separated by NdO rock-salt type layers (Fig. 1). The parent structure $Nd_4Ti_4O_{14}$ is the most oxygen rich, with a composition $NdTiO_{3.5}$. This phase contains Ti^{4+} ($3d^0$) and is a ferroelectric insulator with extremely high Curie temperature (>1500 °C) that could have applications as high temperature transducers and high-K microwave dielectrics. As the thickness of the layers (n) increases, the composition moves towards $NdTiO_3$. Concurrently, the dimensionality of the structures moves from the 2-dimensional layered material $NdTiO_{3.5}$ towards the 3-dimensional perovskite $NdTiO_3$. This material has Ti in a Ti^{3+} ($3d^1$) state, and is insulating with ferromagnetic properties [10]. For the material $NdTiO_{3+\delta}$, both ferromagnetic properties vanish and an insulator-to-metal transition occurs for $\delta > \sim 0.1$, while still maintaining the parent (3D) perovskite structure. [11]. As remarked, above $\delta \sim 0.15$, the layered $Nd_nTi_nO_{3n+2}$ phases begin to appear. An interesting question to be addressed is how the electrical properties change as the oxygen content (nominal Ti valence or more correctly the charge distribution) varies between 3.00 and 3.5. Studies of the electrical properties of systems where there is a crossover from 2-dimensional to 3-dimensional structures generally show that the conductivity increases with the dimensionality [12,13]. Conductivity measurements on the closely related $La_nTi_nO_{3n+2}$ system show a large increase in conductivity of $La_5Ti_5O_{17}$ compared to $La_4Ti_4O_{14}$ [14,15].

In view of the fact that for the $Nd_nTi_nO_{3n+2}$ system values of $n > 5$ were reported, whereas only $n = 4$ and $n = 5$ (plus intergrowths between them) have been reported for the corresponding La system, we have prepared, by the arc-melting technique, phases with nominal compositions $n = 4.5$, 5, 5.5, 6, and 6.5.

* Corresponding author. Present address: School of Science and Computing, I.T. Tralee, Co. Kerry, Ireland.
E-mail addresses: e.j.connolly@umail.ucc.ie, e_connolly@hotmail.com (E.J. Connolly).

0925-8388/$ – see front matter © 2011 Elsevier B.V. All rights reserved.
doi:10.1016/j.jallcom.2011.11.044

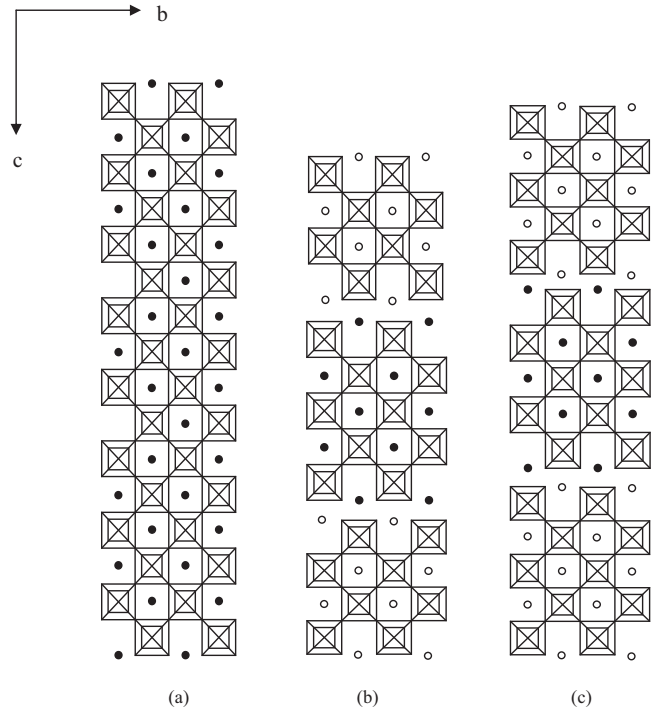

Fig. 1. Schematic view of undistorted $Nd_nTi_nO_{3n+2}$ structures along the *a*-axis: (a) $n=\infty$ (the *c*-axis is parallel to the perovskite [1 1 0] direction), (b) $n=4.5$ (a regular intergrowth structure with stacking sequence $n=4, 5, 4, 5, 4, 5,\ldots$), (c) $n=5$. The squares represent the TiO_6 octahedra and the circles represent the Nd cations. The light circles in (b) and (c) signify that these perovskite slabs are raised/lowered out of the drawing plane by half an octahedra body diagonal (~0.2 nm). Typically the structures are distorted by tilting of the TiO_6 octahedra and displacements of the Nd cation at the interface between adjacent perovskite slabs.

2. Experimental

The starting materials were Nd_2O_3, ex Alfa industries (99.99%) and Johnson Matthey "Specpure" grade TiO_2 and Ti sponge. In all preparations the Nd_2O_3 and TiO_2 powders were dried at 900 °C and weighed rapidly so as to minimise composition drift due to water absorption, especially by Nd_2O_3. Samples of nominal composition $Nd_nTi_nO_{3n+2}$ with $n=4.5$, 5, 5.5, 6, and 6.5 were made by weighing out appropriate amounts of these chemicals, mixed in an agate mortar and then pressed in a die at a pressure of 900 bar into 1-cm diameter pellets. The resultant pellets were arc-melted on a water-cooled copper hearth under flowing argon. The global composition of the samples was determined gravimetrically by oxidation to $Nd_4Ti_4O_{14}$ in air at 1000 °C.

After reaction part of each sample was examined by powder X-ray diffraction using a Guinier–Hägg focusing camera (Expectron XDC-1000) employing strictly monochromatic Cu*K*1 radiation and KCl as an internal standard ($ao=6.2923$ Å at 25 °C). Lattice parameters were refined using standard least squares techniques [16,17]. X-ray diffraction data for other samples were examined via a Siefert model XRD 3000TT diffractometer. Reflections obtained were compared with PDF data [18–21].

Electrical resistance of the samples was measured from 77 K to 300 K using a standard four-probe method. For the purpose of these measurements, the arc melted beads were ground on two parallel faces using standard wet/dry grinding/polishing techniques. Resistance measurements were performed using an evacuated Oxford Instruments type CF1104 cryostat, with an ITC-500 temperature controller. The sample temperature was held at the set-point temperature for about 30 min before taking any measurements, to ensure that thermal equilibrium had been established. A test current supplied by a Keithley type 224 constant current source was monitored via a Keithley type 181 nanovoltmeter. The temperature was monitored by means of an Au-0.3%Fe/Chromel thermocouple. The whole process was automated and monitored by purpose-written software.

3. Results

3.1. X-ray powder pattern phase analysis

Images of the X-ray films obtained from our samples are shown in Fig. 2(b)–(f), and can be compared with a simulation of the literature [18] diffraction pattern, shown in Fig. 2(a). None of the powder diffraction patterns could be indexed uniquely and it is concluded that the arc-melted samples were generally multiphasic. Nevertheless, X-ray patterns were able to provide an overall phase analysis and confirmed that our arc-melted samples had a similar, monoclinic, crystal structure to those reported in the literature [10]. As can be seen, the X-ray powder pattern recorded for the nominal composition $n=4.5$ was found to correspond, with slightly altered *d*-values, to that recorded in the literature for $Nd_4Ti_4O_{14}$. Some of the reflections obtained for the $n=4.5$ sample could be indexed and the corresponding *d*-values are tabulated, along with the PDF *d*-values for $Nd_4Ti_4O_{14}$, in Table 1.

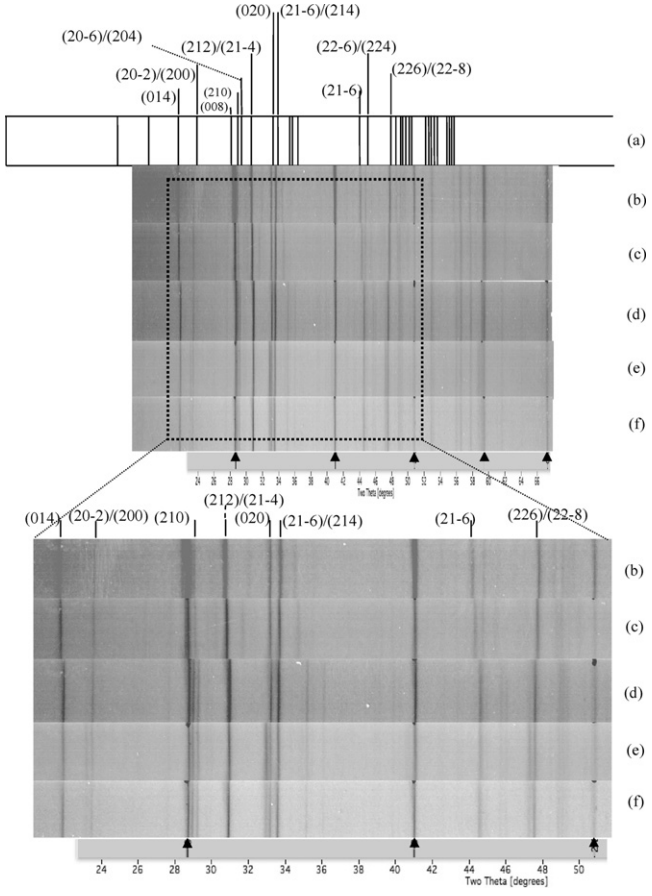

Fig. 2. (a) PDF simulation for $Nd_4Ti_4O_{14}$ [18]; X-ray powder diffraction images for (b) $NdTiO_{3.476}$, (c) $NdTiO_{3.449}$, (d) $NdTiO_{3.414}$, (e) $NdTiO_{3.376}$, and (f) $NdTiO_{3.368}$. The black triangles below indicate KCl internal reference lines. The outlined region is enlarged below for clarity.

Table 1
Indexing of $n=4.5$ compared to the PDF data.

PDF $Nd_4Ti_4O_{14}$ ($n=4$) diffraction pattern ref. [18]		observed $n=4.5$ preparation diffraction pattern	
d-spacing [Å]	*h k l*	*d*-spacing [Å]	Obs. difference [Å]
4.162	0 1 4	3.995	−0.167
3.797	2 0 −2/2 0 0	3.765	−0.032
3.119	2 1 0/2 1 −2	3.113	−0.006
3.077	2 0 −6/2 0 4	3.075	−0.002
2.950	2 1 2/2 1 −4	2.905	−0.045
2.732	0 2 0	2.705	−0.027
2.681	2 1 −6/2 1 4	2.652	−0.029
2.043	2 2 −6/2 2 4	2.024	−0.019
1.9043	2 2 6/2 2 −8	1.9045	+0.0002

Table 2
XRD phase analysis showing reflections present based on respective ICSD PDF files refs. [18–21] for the $Nd_nTi_nO_{3n+2}$ preparations: $n = 4.5–6.5$.

Nominal n	Composition (after oxidation)	$Nd_4Ti_4O_{14}$	$Nd_5Ti_5O_{17}$ (based on $La_5Ti_5O_{17}$)	$NdTiO_3$	Nd_2TiO_5
4.5	$NdTiO_{3.476}$	(0 1 4)→ (2 0 −2)/(2 0 0)→ (2 1 0)/(2 1 −2) (2 0 −6)/(2 0 4) (2 1 2)/(2 1 −4)→ (0 2 0)→ (2 1 −6)/(2 1 4)→ (2 2 −6)/(2 2 4)← (2 2 6)/(2 2 −8)	(0 1 5)→ (2 0 −2)→ (0 0 10) (2 0 8) faint (2 2 6) (2 1 −13)/(2 1 11)→	(2 2 1) (0 2 0) very faint	(0 3 1) (4 0 0) (4 1 0) very faint
5	$NdTiO_{3.449}$	(0 1 4)→ (2 0 −2)/(2 0 0)→ (0 1 6) very faint (0 0 8) very faint (2 1 0)/(2 1 −2) (2 0 −6)/(2 0 4)→ (2 1 2)/(2 1 −4)→ (0 2 0)→ (2 1 −6)/(2 1 4)→ (2 2 −6)/(2 2 4) (2 2 6)/(2 2 −8)←	(0 1 5)→ (2 0 −2)→ (0 0 10)→ (2 0 8)→ faint (2 2 6)→ (2 1 −13)/(2 1 11)→	(2 2 1)←	(0 3 1) (4 0 0)
5.5	$NdTiO_{3.414}$	(0 1 4)→ (2 0 −2)/(2 0 0)→ (0 0 8) very faint (2 0 −6)/(2 0 4) (2 1 2)/(2 1 −4)→ (0 2 0)→ (2 1 −6)/(2 1 4)→ (3 0 −2)/(1 0 −10)→ (4 0 −2) very faint (2 2 6)/(2 2 −8)←	(0 1 5)→ (2 0 −2)→ (0 1 11) (2 1 −13)/(2 1 11) (0 1 15) faint (0 2 12) very faint→	(2 2 1)← (2 2 0)← (0 0 4)← faint	(2 3 0) (0 3 1) (4 0 0)
6	$NdTiO_{3.376}$	(0 1 4)→ (2 0 −2)/(2 0 0)→ (0 0 8) very faint (2 0 −6)/(2 0 4) (2 1 2)/(2 1 −4)→ (0 2 0)→ (2 1 −6)/(2 1 4)→ (3 0 −2)/(1 0 −10)→ (4 0 −2) (2 2 6)/(2 2 −8)←	(0 1 5)→ (2 0 −2)→ (0 1 11) (2 1 −13)/(2 1 11) (0 1 15) very faint (0 2 12)→	(2 2 0)← (0 0 4)← faint	(2 3 0) (0 3 1) (4 0 0)
6.5	$NdTiO_{3.368}$	(0 1 4)→ (2 0 −2)/(2 0 0)→ (0 0 8) very faint (2 0 −6)/(2 0 4) (2 1 2)/(2 1 −4)→ (0 2 0)→ (2 1 −6)/(2 1 4)→ (3 0 −2)/(1 0 −10)→ (4 0 −2) faint (2 2 6)/(2 2 −8)←	(0 1 5)→ (2 0 −2)→ (0 1 11) (2 1 −13)/(2 1 11) (0 1 15) very faint (0 2 12)→	(2 2 0)← (0 0 4)← very faint	(2 3 0) (0 3 1)← (4 0 0)←

→/← indicates observed reflections are shifted right/left relative to ICSD PDF data.

Table 2 shows a summary of the phase analysis. Small amounts of Nd_2TiO_5 seem to be present in all the patterns, but the amount seems approximately constant. Similarly, small amounts of $NdTiO_3$ seem to be present.

Powder patterns for the nominally prepared $n = 4.5$, 5, 5.5, 6, and 6.5 samples were all basically similar to each other. Each retained the (0 1 4), (2 0 −2)/(2 0 0), (2 0 −6)/(2 0 4), (−2 1 2)/(2 1 −4), (0 2 0), (2 1 −6)/(2 1 4), (2 2 −6)/(2 2 4) and (2 2 6)/(2 2 −8) reflections found in the $Nd_2Ti_2O_7$ pattern, with increasingly altered d-values (as n increased). There seemed to be a slight shift of some of these powder diffraction pattern lines to the right, possibly indicating a decrease in unit cell volume as oxygen is removed from $NdTiO_{3.5}$, similar to that described for increasing δ in $NdTiO_{3+\delta}$ [11]. A reflection indexed as (2 1 0)/(2 1 −2) appeared in samples with nominal composition $n = 4.5$ and $n = 5$. Other reflections appearing across the series were: (0 1 6) (in $n = 5$ composition), (0 0 8) (in $n = 5$, 5.5, 6, and 6.5 compositions), and (3 0 −2)/(1 0 −10), (4 0 −2) (in $n = 5$, 5.5, and 6 compositions). The (0 0 2) reflection, and many other reflections with an 0 0 l component were weak or absent. A line indexed as (0 0 10) from the $Nd_5Ti_5O_{17}$ phase [19] is present in $n = 4.5$ and $n = 5$ compositions, but is absent in $n = 5.5$, 6 and 6.5 compositions. A line indexed as (0 1 11) appears in $n = 5.5$, 6 and 6.5 compositions. Similarly, a line indexed as (0 2 12) appears very weakly in $n = 5.5$, and is stronger in $n = 6$ and $n = 6.5$ compositions.

The conclusions to be drawn from the X-ray analysis is that the preparations are multiphasic, but that the trend is to pass along the series from $Nd_4Ti_4O_{14}$ towards $Nd_6Ti_6O_{20}$ as anticipated.

3.2. Oxidation to determine oxygen content of made samples

The global composition of most samples was determined gravimetrically by oxidation to $Nd_4Ti_4O_{14}$ in air at 1000 °C. Table 3 shows the value of n aimed for, with both the nominal and made

Table 3
Preparations for the $Nd_nTi_nO_{3n+2}$ system and summary of resistance measurements; $n = 4.5–6.5$.

Nominal composition	n[a]	Composition (after oxidation)	Δ[b]	R (300 K) [Ω]	R (75 K) [Ω]	E_a[d] [meV]
$NdTiO_{3.44}$	4.5	$NdTiO_{3.476}$	0.036	~15	~200	~67 (HT); ~17 (LT)
$NdTiO_{3.40}$	5	$NdTiO_{3.449}$	0.049	~40	~3000	~39
$NdTiO_{3.36}$	5.5	$NdTiO_{3.414}$	0.054	~5	11.5	~8.6
$NdTiO_{3.33}$	6	$NdTiO_{3.376}$	0.046	0.097	0.11	~0.086
$NdTiO_{3.307}$	6.5	$NdTiO_{3.368–3.393}$[c]	0.061–0.086[c]	0.004	0.098	~140 (HT); ~9.48 (LT)

[a] n = the number of TiO_6 octahedral layers.
[b] Δ is the excess oxygen of the prepared samples compared to the nominal compositions.
[c] 'Oxidation' of different parts of the same sample, showing a spread of ~0.02.
[d] E_a is the activation energy estimated from the slope of lnR *v.* $1/T$ plots; some samples showed a change in the activation energy with temperature: HT and LT stand for high ($T > 200$ K) and low ($T < 200$ K) temperatures respectively.

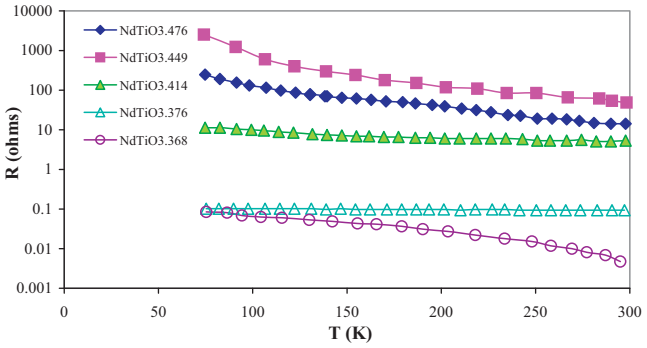

Fig. 3. Resistance–temperature data between 75 K and 300 K for $NdTiO_{3.476}$ ($n = 4.5$ preparation), $NdTiO_{3.449}$ ($n = 5$ preparation), $NdTiO_{3.414}$ ($n = 5.5$ preparation), $NdTiO_{3.376}$ ($n = 6$ preparation) and $NdTiO_{3.368}$ ($n = 6.5$ preparation).

compositions, and the excess oxygen Δ, for preparations of $Nd_nTi_nO_{3n+2}$. As with $NdTiO_{3+\delta}$ materials [11], the final compositions typically had ~0.05 excess oxygen.

3.3. Electrical conductivity

A summary of the electrical conductivity results is shown in Table 3, and Fig. 3. It can be seen that as n is increased, (or, as oxygen is removed from $Nd_4Ti_4O_7$), there is an overall decrease in the measured resistances, R (300 K) and R (75 K). Activation energies, E_a, of the form $\rho \sim \exp(-E_a/k_BT)$ were extracted from the slope of $ln(1/R)$ *v.* $1/T$ plots and are also tabulated with the conductivity data in Table 3. Values of E_a show a decrease with increasing n (i.e. with increasing dimensionality).

4. Discussion

The decrease in resistance (or equivalently, the increase in conductivity) with increasing dimensionality is consistent with other work on similar materials [12–15]. Samples with $n = 6$ were found to form more readily within the $Nd_nTi_nO_{3n+2}$ system, compared to the corresponding $La_nTi_nO_{3n+2}$ system. Thus, the increased ability to form phases with higher values of n has been attributed to the fact that Nd has a smaller ionic radius than La [22].

In the compound $NdTiO_{3.5}$, or $Nd_4Ti_4O_{14}$, the crystal structure is composed of 4-octahedra-thick layers, sandwiched between rock-salt-type layers of NdO_2. For this crystal structure an ionic model would predict that $Nd_4Ti_4O_{14}$ is an insulator because local charge balancing requires Ti to exist as Ti^{4+}. This would imply that the d-electron levels are empty ($3d^0$). An elementary band-theory approach would suggest that $Nd_4Ti_4O_{14}$ is an insulator because there is an energy gap, E_g, between bands formed from the 'full' O-2p and 'empty' Ti-3d levels. When the composition is changed to $NdTiO_{3.4}$, which forms as $Nd_5Ti_5O_{17}$, the *average* Ti valence must be $Ti^{3.8+}$. Assuming that the only important difference in crystal structures between $Nd_4Ti_4O_{14}$ and $Nd_5Ti_5O_{17}$ – as far as electrical conductivity is concerned – is the thickness of the octahedral layers, then the value of E_g would be expected to be similar for the two structures.

The decrease in resistance as n increases, measured for our samples, might be then rationalised as either holes forming in an O-2p valence band, or, with the formation of delocalised Ti^{3+}, possibly by 3d band conduction or by hopping conduction.

Values of activation energies are similar to those observed for other isostructural layered systems [5], where it was also observed that a decrease in activation energies often occurred at lower temperatures ($T < 150$ K).

Resistance measurements on single-crystal samples generally reveal a higher resistance, or lower conductivity in the c-direction compared to the a- and b-directions, caused by the anisotropy in the crystal structure [5]. Due to the multi-phase nature of our samples it is expected that our resistance measurements will be dominated by the electrical properties of the c-direction (i.e. higher resistivity pathways). This could explain why a sample with composition $NdTiO_{3.376}$ was found to have negligible activation energy (0.086 meV) but still had increasing resistance for decreasing temperature, typical of semiconducting or insulating behaviour. Single crystal samples of $La_5Ti_5O_{17}$, and other $n = 4$ and $n = 5$ materials [5] show anisotropic electrical conductivities with insulating or semiconducting behaviour for the c- and b-directions and metallic or almost metallic behaviour for the a-direction, with activation energies in the range 0.5–58 meV. Such quasi-1-dimensional metals, which can simultaneously display high dielectric polarisability in the c-direction with semiconducting properties in the b-direction and metallic conductivity in the a-direction are very interesting for their electrical, magnetic and optical properties. Lichtenberg et al. [5] suggest that this quasi-1-dimensional metallic behaviour is dependant on the distortion of the BO_6 octahedra within the perovskite layers, with more pronounced 1-dimensional metallic behaviour for more distorted octahedra. A structural characterisation of $Nd_5Ti_5O_{17}$ [9] found that the TiO_6 octahedra were significantly more distorted than in $La_5Ti_5O_{17}$ (most likely due to the smaller Nd ion), which could imply that if careful measurements were made on single-crystal samples, the Nd material could have more pronounced 1-dimensional electrical properties, allowing a clearer understanding of 1-dimensional electrical and magnetic phenomena.

Often it is required for applications to have materials with different properties in close proximity. For example, capacitive based sensors usually require high conductivity sensing electrodes separated by a dielectric sensing material. Or perhaps magnetic-based systems may require magnetic and non-magnetic materials to be in close proximity. The 'proximity' of these properties (structurally and compositionally) is likely to be utilised especially by systems which need 'integrated properties', perhaps sensor systems such as layered metal/insulator/metal nanostructures such as $Nd_nTi_nO_{3n+2}$

phases with $n = \infty/n = 4/n = \infty$ (the phase $n = \infty$ with a small amount of excess oxygen is metallic [11]), or $Nd_nTi_nO_{3n+2}$ phases with $n = 4/n = 6/n = 4$ to form insulator/1-dimensional metal/insulator structures for use as improved selectivity gas sensors, or for materials/systems with electric-field controlled charge carrier density [23].

Acknowledgement

EJC is indebted to the School of Engineering, University of Cardiff, for a grant which made this study possible.

References

[1] B. Jaffe, W.R. Cook, H. Jaffe, Piezoelectric Ceramics, Academic Press, New York, 1972.
[2] J.B. Goodenough, J. Mater. Educ. 9 (6) (1987) 619.
[3] Physics Today, June 1991.
[4] P.A. Cox, Transition Metal Oxides, Clarendon Press, Oxford, 1992.
[5] F. Lichtenberg, A. Herrnberger, K. Wiedenmann, J. Mannhart, Prog. Solid State Chem. 29 (2001) 1–70.
[6] J. Sloan, R.J.D. Tilley, Eur. J. Solid State Inorg. Chem. 31 (1994) 673.
[7] J. Sloan, R.J.D. Tilley, J. Solid State Chem. 121 (1996) 324.
[8] E. Connolly, J. Sloan, R.J.D. Tilley, Eur. J. Solid State Inorg. Chem. 33 (1996) 371.
[9] M. Sayagues, K. Titmuss, R. Meyer, A. Kirkland, J. Sloan, J. Hutchison, R.J.D. Tilley, Acta Cryst. B59 (2003) 449.
[10] C. Eylem, H.L. Ju, B.W. Eichorn, R.L. Green, J. Solid State Chem. 114 (1995) 164.
[11] E.J. Connolly, R.J.D. Tilley, A. Arulraj, R. Gundakaram, C.N.R. Rao, J. Alloys Compd 388 (2005) 153.
[12] R.A. Mohan, P. Ganguly, C.N.R. Rao, J. Solid State Chem. 70 (1987) 82.
[13] R.A. Mohan, P. Ganguly, C.N.R. Rao, J. Solid State Chem. 63 (1986) 139.
[14] F. Lichtenberg, D. Widmer, J.G. Bednorz, T. Williams, A. Reller, Z. Phys. B 82 (1991) 211.
[15] F. Lichtenberg, T. Williams, A. Reller, D. Widmer, J.G. Bednorz, Z. Phys. B 84 (1991) 369.
[16] P.-E. Werner, Ark. Kem. 31 (1969) 513.
[17] P.A. Stadelmann, Ultramicroscopy 21 (1987) 131.
[18] PDF $Nd_4Ti_4O_{14}$: ICDS entry 4133.
[19] PDF $La_5Ti_5O_{17}$: ICDS entry 281282.
[20] PDF $NdTiO_3$: ICDS entry 8147.
[21] PDF Nd_2TiO_5: ICDS entry 247560.
[22] M. Nanot, F. Queyroux, J.-C. Gilles, R. Portier, M. Fayard, Mater. Res. Bull. 10 (1975) 313.
[23] A.D. Caviglia, S. Gariglio, N. Reyren, D. Jaccard, T. Schneider, M. Gabay, S. Thiel, G. Hammerl, J. Mannhart, J.-M. Triscone, Nature 456 (2008) 624.